engineering proceedings

Proceedings Paper

Optical Investigation of PVA/PbTiO$_3$ Composite for UV Protective Approaches Applications [†]

A.S. El-Deeb [1], M.M. Abdel Kader [1], G. M. Nasr [2], M. A. Ahmed [3] and Eman O. Taha [3,*]

[1] Housing and Building National Research Center, Building physics Institute, Giza 1770, Egypt; asmaphysics@yahoo.com (A.S.E.-D.); marwamahmoud_1211@yahoo.com (M.M.A.K.)
[2] Faculty of Science, Department of Physics, Cairo University, Giza 12613, Egypt; rrrrrgmal@yahoo.com
[3] Egyptian Petroleum Research Institute (EPRI), Department of Petroleum Applications, Cairo 11727, Egypt; mona_chemist17@yahoo.com
* Correspondence: eman@unm.edu; eman.omar@epri.sci.eg

† Presented at the 2nd International Electronic Conference on Applied Sciences, 15–31 October 2021; Available online: https://asec2021.sciforum.net/.

Abstract: New-fangled polymer of poly(vinyl Alcohol) (PVA) doped with various concentrations of lead(II) Titanate (PbTiO$_3$, PT) are prepared using casting technique method. The prepared samples are identified by Attenuated Total Reflection- Fourier Transform Infrared (ATR-FTIR). The peaks characterized to PVA at 3280, 2917, 1690, 1425, 1324, 1081, 839 cm^{-1} appeared, also the peak characterized to the presence of PbTiO$_3$ appeared at 713 cm^{-1}. The interaction between PVA and PbTiO$_3$ was confirmed by observing the change in IR absorption intensity. Optical properties UV-Vis range was investigated using Ultraviolet Visible technique (UV-Vis). An enhancement in absorption capacity by the increasing PbTiO$_3$ concentration was observed. Optical properties such as band gap energy, Urbach energy, extinction coefficient indicate that addition of PbTiO$_3$ into PVA polymer induced variance in internal states by increasing the ratio of PbTiO$_3$.

Keywords: PVA; PbTiO$_3$; optical properties

Citation: El-Deeb, A.S.; Kader, A.; Nasr, G.M.; Ahmed, M.A.; Taha, E.O. Optical Investigation of PVA/PbTiO$_3$ Composite for UV Protective Approaches Applications. **2021**, 3, x. https://doi.org/10.3390/xxxxx

Academic Editor: Nicholas Sarlis

Received: date
Accepted: date
Published: 15 October 2021

1. Introduction

Polymeric nanocomposite materials have gotten a lot of attention lately because of the expanded range of applications that these hybrid materials can be used for [1]. It is widely documented that polymers, as dielectric materials, are good host matrices for nanoparticles [2], and that this is true for both metal and ceramic nanoparticles. While doing so, these embedded particles within the polymer matrix will also impact the physical properties of the host [3,4]. Polymer ceramic hybrid composites, in particular, are promising functional materials in a variety of disciplines, including optical, electrical, thermal, mechanical, and antibacterial characteristics [4].

Composites made of piezoelectric ceramics such as barium titanate (BT), lead titanate (PT), triglycine sulphate (TGS), and lead zirconate titanate (PZT) etc. have been studied extensively [5]. Lead titanate (PbTiO$_3$) is a ferroelectric ceramic that shares the perovskite family with barium titanate and lead zirconate titanate. All of these materials have one or more phase transitions within a particular temperature range. However, lead titanate exhibits the largest spontaneous polarization in the tetragonal phase (tetragonality factor c/a = 1.064), the lowest dielectric constant (≈200), and high Curie temperature (≈490 °C)[6].

Polyvinyl alcohol (PVA) is a polymer with good film-forming and physical properties, high hydrophilicity, processability, biomaterial, and biosensor qualities [7,8]. PVA is a semicrystalline polymer (Cryo-Amorphous) made up of both crystalline and amorphous phases. When such a polymer is mixed with a suitable ceramic, it interacts either in the amorphous or crystalline fractions, affecting the physical quantities in both cases [9].

It is reported in this study that the preparation and investigation of the optical properties of PVA/$PbTiO_3$ composite films were carried out because these films can combine the advantages of both polymers and ceramics components.

2. Experimental

Polyvinyl alcohol (PVA) powder and Lead (II) titanate ($PbTiO_3$) powder were supplied from Sigma- Aldrich. PVA was dissolved in double-distilled water at 80 °C and stirred for 4 h to ensure uniform dispersion. To prepare $PbTiO_3$/PVA composites, different weight percentages (0, 1, 5, and 10 wt%) are added to the above solution of PVA in water and stirred for 1 h. The mixture was then cast in a glass dish, and the sample was left to dry for a week at room temperature. The dispersion state of the prepared samples was examined using Field Emission Scanning Electron Microscope (FESEM Sigma 300 VP, Carl Zeiss, Germany). Figure 1 shows the FESEM micrograph for 10 wt% $PbTiO_3$ in the PVA. The image demonstrate the absence of aggregation of $PbTiO_3$ and its homogenous dispersion.

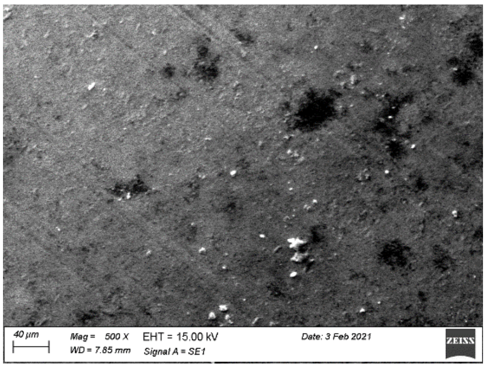

Figure 1. FESEM of 10 wt% $PbTiO_3$/PVA composite.

Alpha Bruker platinum Attenuated Total Reflection-Fourier Transform Infrared Spectroscope (ATR-FTIR) with wavenumber range of 600–4000 cm^{-1} were determined for characterization of polymer composite. UV-Vis spectra were measured using Jasco V-630 spectrophotometer.

3. Results and Discussion

3.1. ATR-FTIR

ATR-FTIR spectroscopy provides a key approach for identifying and characterizing polymer composites. The PVA/$PbTiO_3$ composite ATR-FTIR spectra with various $PbTiO_3$ contents are illustrated in Figure 2. The major peaks of PVA were found at 3280 cm^{-1}, indicating the presence of O-H stretching vibration of the hydroxyl group. Peak at 2917 cm^{-1} linked with the existence of the asymmetrical deep vibration of CH. The peak at 1690 cm^{-1} for C=O carbonyl stretch. The peak at 1425 cm^{-1} for bending vibration of CH_2 [10]. The peaks at 839 cm^{-1}, 1081 cm^{-1}and 1324 cm^{-1} were associated to C-C stretching vibration, vibration C-O stretching of acetyl groups and the presence of C-H deformation [11]. For PVA/$PbTiO_3$ composite several peaks occurred, with a belt additive of 713 cm^{-1} indicating a metal oxygen stretching, which in turn shows the presence of a metal oxygen bonds.

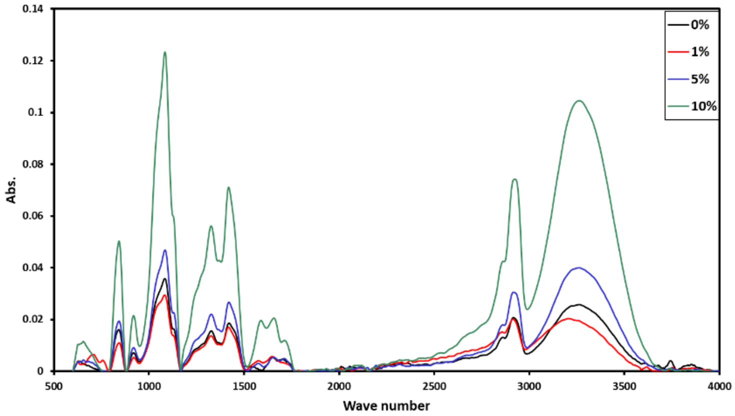

Figure 2. ATR-FTIR spectra for PVA/$PbTiO_3$ composite.

3.2. Optical Properties

Ultraviolet visible spectroscopy is one the most prevalent mechanisms that can detect every molecule, identify functional groups and emphasize the concentration of analytes that is indicated by absorbance using Beer's law. UV-Vis absorption spectrum of PVA/$PbTiO_3$ with (0, 1%, 5%, 10%) $PbTiO_3$ concentrations are depicted in Figure 3. Absorption peaks obtained from 350 to 450 nm for 5% & 10% $PbTiO_3$ due to the energy of the forbidden band conformable to O-2p→Ti-3d. While no peaks are obtained neat PVA or 1% $PbTiO_3$ concentration. The intensity of absorption decreases with wavelength increase for all samples. High absorption is obtained in the UV region for samples with 5% and 10% concentration that qualify them to be promising in UV protective approaches.

In low and poor crystalline materials, disordered and amorphous materials exponential tails appear near the optical edge called Urbach tail due to the localized states that the materials have. This localized states prolonged in the band gap and can be described by Urbach rule [12].

$$\alpha = \alpha_o \; exp\left(\frac{h\gamma}{E_u}\right) \tag{1}$$

While α is the absorption coefficient, $h\gamma$ is the photon energy, α_o is a constant and E_u is the band tail energy (Urbach energy), that is weakly temperature dependence and interpreted as the band tail width due to the localized states placed inside band gap that is associated with low and poor crystalline materials, disordered and amorphous materials, Figure 4 depict the relation between the absorption coefficient α and the photon energy E($h\gamma$),whereas the slope of the straight line after taking the logarithm of Equation (1) gives Urbach energy (E_u), then it is essential to take the logarithm of Equation (1) [12]:

$$ln\,\alpha = ln\,\alpha_o + \left(\frac{h\gamma}{E_u}\right) \tag{2}$$

And plotting $\ln\alpha$ against the incident photon energy $h\gamma$ in Figure 5.

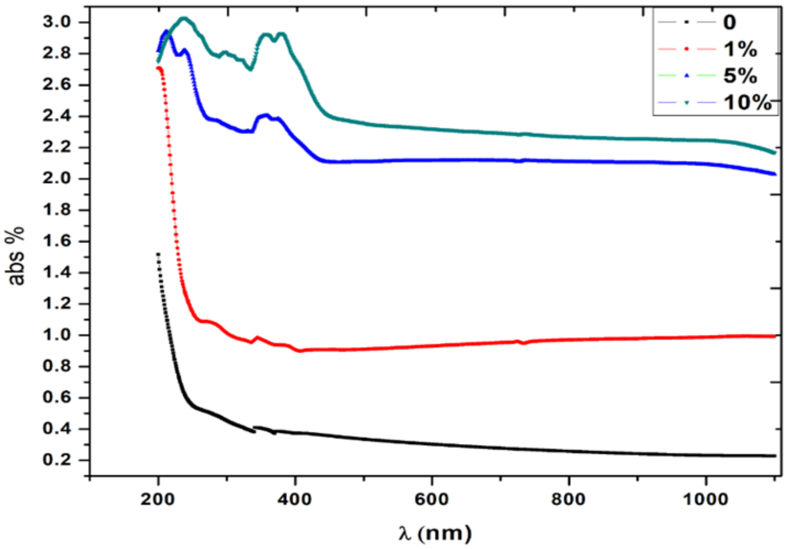

Figure 3. UV-Vis spectra of PVA/$PbTiO_3$ composite.

Transition of electrons can take place in semiconductor materials between valance band and conduction band. Spontaneous emission, absorption and simulated emission can take place between conduction band and valance band. Band gap energy can be determined by plotting $(\alpha h\gamma)^{1/K}$ and $h\gamma$ where K depends on the transition nature. For direct transition K = ½ through this direct transition electron that rises from valance band to conduction band changes only its potential, while for indirect transition $K = 2$ electron that rises form valance band to conduction band changes potential and momentum. The direct and indirect transition can be described by the equation [13]:

$$(\alpha h\gamma) = B\ (h\gamma - E_g)^{1/k} \quad (3)$$

B is a constant depend on the transition probability. Figure 6 shows the plot of $(\alpha h\gamma)^2$ and $(\alpha h\gamma)^{1/2}$ versus $E\ (h\gamma)$ for PVA/$PbTiO_3$ composite. Values of direct and indirect band gap energies are given by the extrapolation of the linear portion of the curve with x-axis. Table 1 indicates the values of absorption edges, band tail energies, indirect (E_i) and direct(E_d) optical band gap for composites. The absorption edge values and the band tail energies decrease with increasing $PbTiO_3$ content. The values of direct and indirect band gaps decrease with increasing $PbTiO_3$ content indicating a variance in internal states. Composite with 10 wt.% is promising for UV protective applications

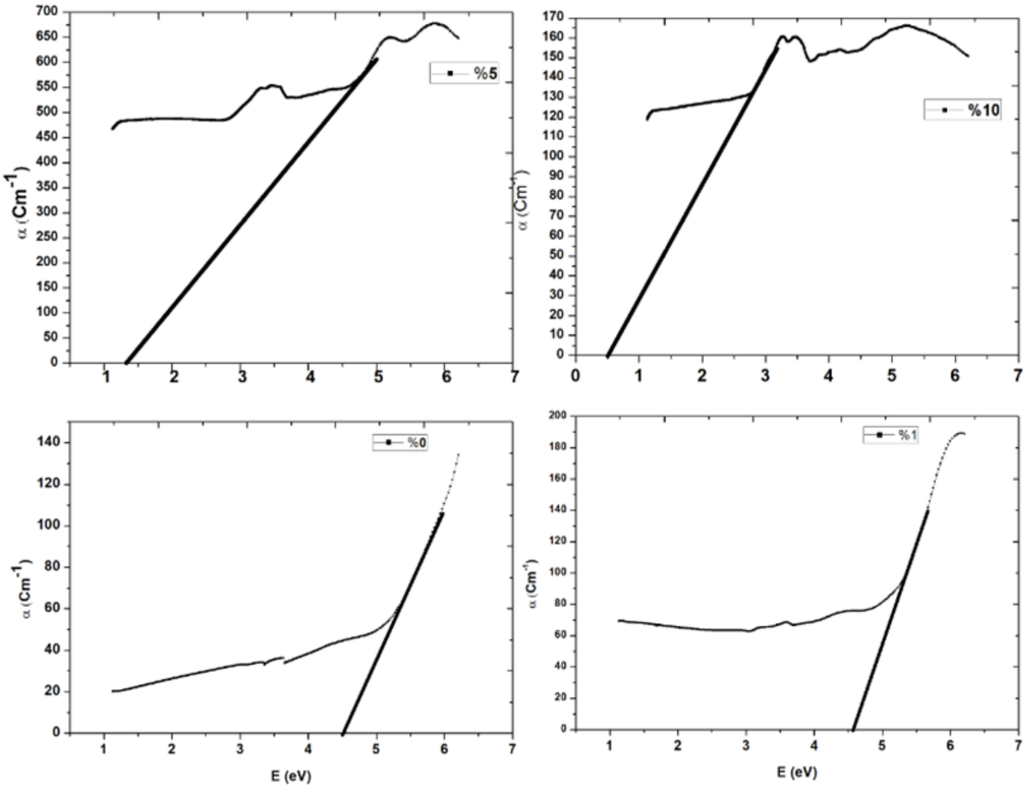

Figure 4. The relation between α and E of PVA/PbTiO$_3$ composite.

Table 1. Values of absorption edge, band tail, indirect (Ei) and direct (Eg) optical band gap energy of PVA/PbTiO$_3$ Composite**.**

PVA/PbTiO$_3$	**Absorption Edge (eV)**	**Band Tail E_u (eV)**	**Energy Gap (eV)**	
			E_i	**E_d**
0%	4.6	1.12	5.3	5.2
1%	4.46	2	5.8	4.8
5%	1.36	2.34	2.8	2.7
10%	0.56	2.74	2.3	2.17

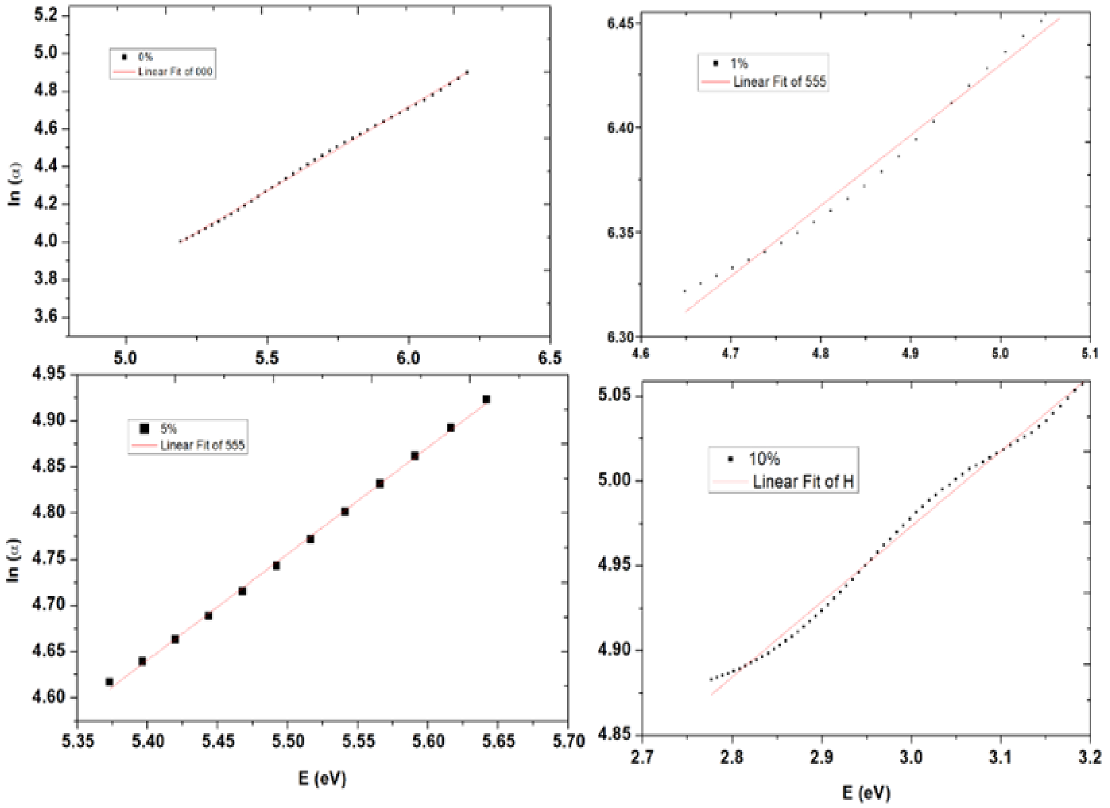

Figure 5. The relation between $\ln \alpha$ and E of PVA/PbTiO₃ composite.

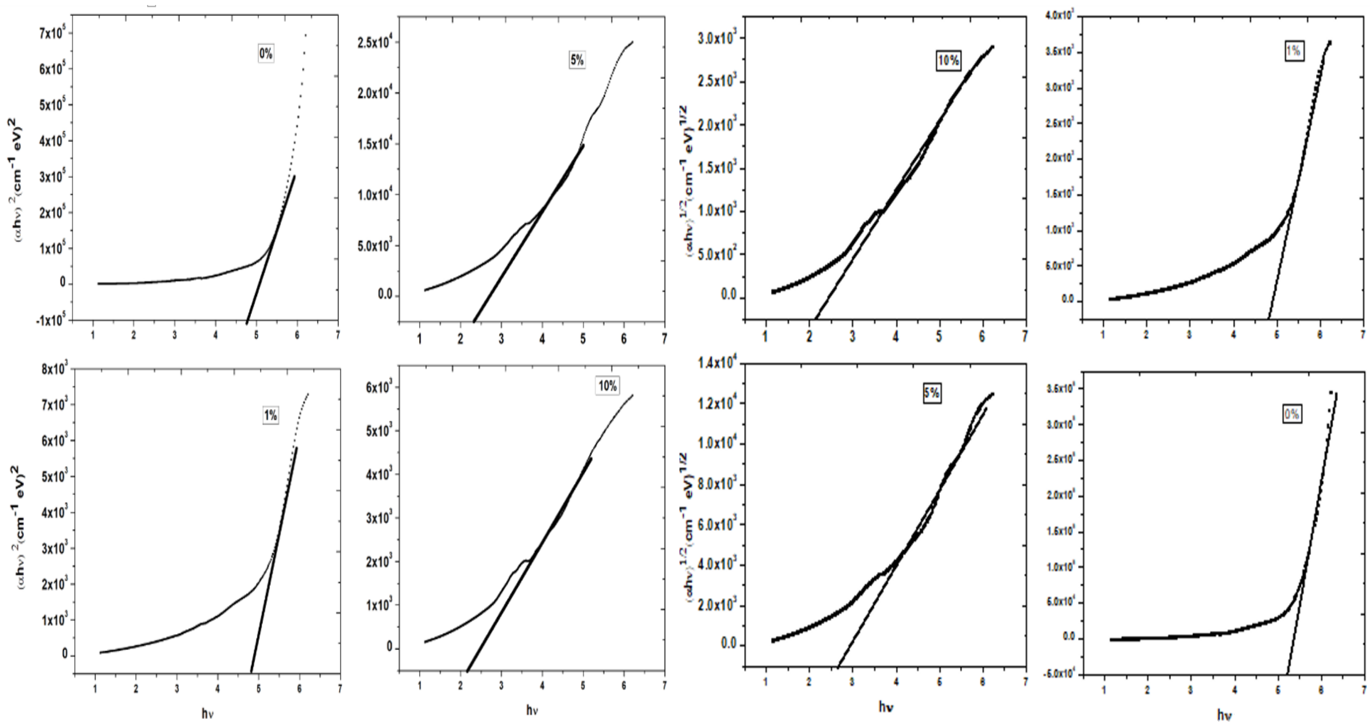

Figure 6. Relation between $(\alpha h\gamma)^2$ and $(\alpha h\gamma)^{1/2}$ against $h\gamma$ for PVA/PbTiO₃ composite.

4. Conclusions

$PVA/PbTiO_3$ composites were prepared using the casting technique method. The absence of aggregations was examined by using FESEM. The peaks characterized PVA appeared when the composites were examined using ATR-FTIR. The absorption edge value and band tail energies decrease with increasing PbTiO3 content. Also, the values of direct and indirect bandgap decrease with increased $PbTiO_3$ content. Composite 10 wt% $PbTiO_3$ is promising for UV protective applications.

Conflicts of Interest: The authors declare no conflict of interest.

References

1. Bailey, E.J.; Winey, K.I. Dynamics of polymer segments, polymer chains, and nanoparticles in polymer nanocomposite melts: A review. *Prog. Polym. Sci.* **2020**, *105*, 101242.
2. Ananth, A.N.; Umapathy, S.; Sophia, J.; Mathavan, T.; Mangalaraj, D. On the optical and thermal properties of in situ/ex situ reduced Ag NP's/PVA composites and its role as a simple SPR-based protein sensor. *Appl. Nanosci.* **2011**, *1*, 87–96.
3. Ghanipour, M.; Dorranian, D. Effect of ag-nanoparticles doped in polyvinyl alcohol on the structural and optical properties of PVA films. *J. Nanomater*. **2013**, *2013*, 1–10.
4. Sebastian, M.T. Polymer–Ceramic Composites of 0–3 Connectivity for Circuits in Electronics: A Review. *Int. J. Appl. Ceram. Technol.* **2010**, *7*, 415–434.
5. Uma, S.; Philip, J. Induction of electro-activity in polyvinyl alcohol with addition of nanocrystalline PZT ceramic. *Int. J. Indian J. Pure Appl. Phys.* **2013**, *5*, 717–723.
6. Mir, M.; de Paula, C.C.; Garcia, D.; Kiminami, R.H.G.A.; Eiras, J.A.; Mascarenhas, Y.P. Microstructural characterization using the Rietveld method in lead lanthanum titanate ceramics. *J. Eur. Ceram.* **2007**, *27*, 3719–3721.
7. Kinadjian, N.; Achard, M.-F.; Julián-López, B.; Maugey, M.; Poulin, P.; Prouzet, E.; Backov, R. ZnO/PVA Macroscopic Fibers Bearing Anisotropic Photonic Properties. *Adv. Funct. Mater* **2012**, 22, 3994–4003.
8. Taha, E.O.; Nasr, G.M. Dielectric and dynamic mechanical properties of Rochelle salt/PVA composites. In *IOP Conference Series Materials Science and Engineering*; IOP Publishing: 2021; p. 12008.
9. Shehap, A.M.; Akil, D.S. Structural and optical properties of TiO_2 nanoparticles/PVA for different composites thin films. *Int. J. Nanoelectron. Mater.* **2016**, *9*, 17–36.
10. Atta, M.M.; Taha, E.O.; Abdelreheem, A.M. Nitrogen plasma effect on the structural, thermal, and dynamic mechanical properties of PVA/starch/graphene oxide nanocomposite. *Appl. Phys. A* **2021**, *127*, 532.
11. Afzal, H.M.; Shehzad, F.; Zubair, M.; Bakather, O.Y.; Al-Harthi, M.A. Influence of microwave irradiation on thermal properties of PVA and PVA/graphene nanocomposites. *J. Therm. Anal. Calorim.* **2020**, *139*, 353–365.
12. Hassaan, M.Y.; Osman, H.M.; Hassan, H.H.; El-Deeb, A.S.;. Al-Helal, M.A. Optical and electrical studies of borosilicate glass containing vanadium and cobalt ions for smart windows applications. *Ceram. Int.* **2017**, *43*, 1795–1801.
13. Aziz, S.B.; Rasheed, M.A.; Ahmed, H.M. Synthesis of Polymer Nanocomposites Based on $[\text{Methyl Cellulose}]_{(1-x)}:(CuS)_x$ $(0.02\ M \leq x \leq 0.08\ M)$ with Desired Optical Band Gaps. *Polymers* **2017**, *9*, 194.

.